Journal of the Serbian Chemical Society
JSCS-info@shd.org.rs • www.shd.org.rs/JSCS

ACCEPTED MANUSCRIPT

Journal of the Serbian Chemical Society
JSCS-info@shd.org.rs • www.shd.org.rs/JSCS
J. Serb. Chem. Soc. **00(0)**1-15 (2023)
JSCS–12148
Original scientific paper
Published DD MM, 2023

Synthesis of sodium silicate crystals from rice husk ash

STELLA ADEDUNNI EMMANUEL[1], ALHASSAN ADEKU SALLAU[1]*, OLUWASEYE ADEDIRIN[1], HUSSAIN DOKO IBRAHIM[2], MOHAMMED LAWAL BUGA[2], ANTHONY OKEREKE[2], GERTRUDE NGOZI OZONYIA[2] AND FORTUNE MIEBAKA ALABI[2]

[1]*Chemistry Advanced Research Center, SHESTCO, Abuja, Nigeria, and* [2]*Raw Materials Research and Development Council, RMRDC, Maitama, Abuja*

(Received 26 November 2022; Revised 20 January 2023; Accepted 10 July 2023)

Abstract: The rich husk is an agricultural waste of rice cultivation worldwide, which is highly rich in amorphous silica. Rice husk obtained from Dagiri was pyrolysed at 750 ℃ to give white ash (RHA) which was further treated with acid (ARHA). The ash was reacted with sodium hydroxide at 90 ℃ for 2 *hours* 30 *min* to produce Sodium silicate crystals. Sodium silicates synthesized in the study were characterized with some physicochemical parameters. Their structural and morphological properties were assessed using a Fourier Transform Infra-red spectrophotometer (FTIR), X-ray Diffractometer (XRD) and Scanning Electrode Microscope (SEM). The mineralogical composition of the ash and sodium silicate was investigated with Energy-dispersive X-ray fluorescence (EDXRF) spectrometer. The sodium silicate produced has a melting point of 61 ℃, a pH of 12.03 and appeared as brownish-white to clear-white in colour. The RHA and ARHA from XRD investigation showed patterns which match the mineral phase cristobalite, while that of the sodium silicate XRD patterns match the mineral heptahydrate disodiumtrioxosilicate as the most dominant phase. Rietveld refinement of the XRD pattern for the sodium silicate gave $R_{wp} = 12.81$, $R_{exp} = 5.55$, $\chi^2 = 5.3274$ and GoF = 2.3081 against a dual phase analysis. The sodium crystal-synthesized is suitable for use in cosmetic formulations.

Keywords: acid treated ash, cosmetic, crystal structure, paddy, silica, water glass.

INTRODUCTION

Rice husk is an agricultural waste material produced via the cultivation of rice[1]. Rice production worldwide was pegged at over 952 million tons in 2016 according to a 2018 data report by FAO. The rice husk, which is the outer cover of the rice, accounts for 20 % of the paddy produced annually (about 190 million tons).[2]

*Corresponding author E-mail: mailto:creamysal@yahoo.co.uk
https://doi.org/10.2298/JSC221126040E

The world has seen a tremendous increase in annual rice production in recent years when compared with the previous report of an estimated 40 million tons in 2003. It is regarded as the second most-produced cereal in the world and geographically concentrated in Asia with over 90 % of the world output. While, Nigeria is putting efforts to develop this sector of agricultural produce, the bulk of rice husks generated is mostly sent to landfills, burnt as fuel to generate energy and leading to residual ashes (RHA) containing over 60 % silica content.[3,4]

Rice husk contains high ash content,[5,6] varying from 13 to 29 wt.% depending on the variety, climate, and geographic location. The ash is largely composed of silica (87–97 %) with small amounts of inorganic salts.[6,7] The high ash content can be recovered as amorphous silica.[8] The amorphous nature of silica in rice husk makes it extractable at a lower temperature range of 90 110 °C.[3]

Sodium silicate solutions are complex mixtures of silicate anions and polymer silicate particles with a molar ratio of SiO_2 to $Na_2O > 2$ and are commercially referred to as water glass.[4] The solutions are generated in different grades as characterized by their SiO_2:Na_2O ratios, varying water contents and low viscosity.[9] Sodium silicate is among the alkaline elements silicate which have attracted extensive studies due to their importance in mineralogy, solid-state chemistry and chemical technology. About 12 natural sodium silicates minerals are known to exist and nine of them have been studied structurally.[10] Anhydrous sodium silicate are considered importance raw materials in production of finished products in both inorganic chemistry and technical mineralogy.[11] Some of industrial applications include production of water glass solutions or manufacture of acid-resistant enamel frits, components of refractory cements, steel and alloy castings, electrodes, dyeing, printing, textile auxiliaries as inorganic binders, or builders in washing powders (soap and detergent cake).[11,12,13] Crystalline sodium silicates such as $Na_2Si_2O_5$ have been shown to exhibit high ion-exchange capacity, selectivity and multifunctionality; such as buffering capacity, water softening ability and ability to degrade fats by hydrolysis as such suggested as alternative replacement of sodium tripolyphosphate builder in detergents.[14,15] It has been suggested that soluble sodium silicates play other vital role of corrosion inhibition in many of its applications such as engine antifreeze and detergents.[16] Sodium silicate in surfactants have been applied in detergent technology for pre-flush technology, with the main role of sodium silicate targeted at removal of hardness (Ca^{2+}, Mg^{2+}) which can complex with anionic surfactants making them less reactive or unstable. The silica anions minimize these unwanted charges by sequestering the metals via a precipitation reaction. The silica anion also competes for active, positively-charged sites on the casing and wellbore thereby reversing their surface charge and repelling surfactants.[12] Sodium silicate is also used as a binder in cosmetic products, such as face powders, eyeliners and lipsticks, to give them a smooth and creamy texture. It helps to bind the different ingredients together and prevent them

from separating[17]. Sodium silicate can be used as a thickener in shampoos and conditioners, to improve viscous and consistency. Sodium silicate can also be used as a pH stabilizer in lotions and creams, to help maintain their pH levels. This is important because certain cosmetic ingredients can become less effective or even unstable at certain pH levels. Sodium silicate can be used as a preservative in liquid soaps and facial cleansers, to help prevent the growth of bacteria and other microorganisms. It works by altering the pH level of the product, which makes it less hospitable to microorganisms. Sodium silicate can also be used as a skin protectant in sunscreens and lotions, to help shield the skin from harmful UV rays and other environmental pollutants. It forms a protective film on the skin, which helps to prevent moisture loss and maintain the skin's natural barrier function[18,19].

The work aims to synthesize a sodium silicate crystal from rice husk ash for possible use in the cosmetic industries.

EXPERIMENTAL

Rice husk was obtained from rice mill at Dagiri, Gwagwalada local government of Federal Capital Territory, Abuja-Nigeria Analar grade Sodium hydroxide (NaOH) and hydrochloric acid (HCl) from Sigma Aldrich were used. All solution was prepared with distilled de-ionized water.

Sample Pre-treatment

Rice husk was washed with water to remove sand and dust particles. The washed rice husk was then spread on tray and air dried for 24 hours. Dried rice husk was placed in stainless steel cylinder and ashed at 750 °C for 3 hours in a Carbolite Muffle Furnace available at Sheda Science and Technology Complex (SHESTCO) Abuja. The pyrolyzed sample tagged RHA were weighed (200 g) separately and treated with 1600 mL of HCl (10 % and 20 % v/v) in a Pyrex beaker and heated for 2 hours at 90 °C. The reaction mixtures were filtered and washed repeatedly with distilled deionized water until the filtrate becomes neutral to litmus. The residues designated 10 % ARHA and 20 % ARHA (acid treated RHA) were dried at 105 °C for 12 hours in a carbolite hot air oven and kept in a desiccator for subsequent steps.

Preparation of sodium silicate

Modified method[20] was adopted: 150 g of ARHA was reacted with 1200 mL NaOH (10 % w/v) in a Pyrex beaker and heated at 110 °C for 2 hours 30 minutes. The reaction mixture was filtered and the filtrate concentrated by heating to 2/3 of its original volume. The concentrate was seeded with a pinch of pure sodium silicate crystals to induce rapid crystallization. The sodium silicate crystals formed was separated by decanting the supernatant liquid. The crystal was rinsed with iced cold distilled deionized water and allowed to drain on a filter. The drained crystals were stored in polyethylene container.

Physicochemical characterization of crystal

Determination of sodium oxide content (IS 6773 (2008): The sodium oxide content of crystal obtained was determined by titrating, a dissolved crystal sample with standard hydrochloric acid to pH 4.3 using methyl orange indicator. 5 g sodium silicate crystals were dissolved in 50 mL deionized water and transferred to 100 mL volumetric flask then diluted to mark with deionized water. A 25 mL portion of the solution was titrated against 0.2 M HCl to orange end point colour.

Calculations

$$C_{Na_2O}/\,\% = \frac{V*M*3.1}{w} \quad (1)$$

Where: V is volume of hydrochloric acid used, M is the molarity of the hydrochloric acid and w is the weight of crystal sample

Viscosity measurement

The viscosity of liquid sodium silicate solutions was determined using the Brookfield Rotational Viscometer according to the ASTM D2983. By insertion of number 2 spindle, rotating at 60 rpm at 25 °C in the sodium silicate liquor. The viscosity was read from the display reading. The determination of viscosity of sodium silicate liquor was essential to determine the optimum thickness for effective crystallization of the sodium silicate crystals from its water glass liquor.

Determination of total solid (IS 6773 (2008)

The total solids of liquid silicates were determined by weighing 5 mL (5 g) into a known weight of pre-fired porcelain crucible and placed in a muffle furnace at 1050 °C for 30 mins. A few drops of 30 % hydrogen peroxide were added to prevent spattering. After cooling in a desiccator and the crucible was reweighed. The weight of the residue was taken and the % solids were reported to the nearest 0.01 %.

Determination of silicon dioxide content (IS 6773 (2008)

The SiO_2 content was calculated by subtracting the % sodium oxide from the % total solids.

Sodium silicates are often described by the weight ratio of the silicon dioxide to the sodium oxide, with the sodium oxide as unity. It may be calculated directly by dividing the % SiO_2 content by the % Na_2O content that has been chemically determined.

Determination of pH (ASTM D4972)

A 0.1 % w/v solution of sodium silicate crystal was prepared by dissolving 0.1 g of sodium silicate crystals in 100 mL deionized water. The pH of the sodium silicate liquor and 0.1 % sodium silicate solution was measured using the pH electrode and Orion Versa Star Pro Meter Advanced electrochemistry meter.

Melting Point determination (DIN 53736)

The microscopic hot stage method melting point apparatus by Bristoline was used. a single crystal sample of the sodium silicate was placed on a hot stage and the heater turned on. The temperature at the point the crystal melts was read from the inserted thermometer.

Characterization of crystal

Empyrean pan-analytical XRD (with Cu Kα at λ = 1.54060, Å v=40 VA, I=40 mA and 5 to 74, 2theta angle), EDXRF (Vacuum and Air atmosphere geological sample analysis) and Phenom ProX Scanning Electron Microscope available at the central laboratory of Umar Musa Yar'adua University, Katsina were used to study the crystal structure, mineral composition and morphology of the crystal respectively. Thermo-Scientific Nicolet iS5 FT-IR Spectrometer equipped with iD7 ATR sampler was used to asses any functional group available in the RHA, ARHA and sodium silicate crystal over the range 500–4000 cm^{-1} and resolution of 0.5 cm^{-1}. The Thermal behaviour was investigated by the PerkinElmer MSE-TGA 4000 TGA (30 - 950 °C at 10 °C /min) available at Ahmadu Bello University Zaria.

RESULTS AND DISCUSSION

Physicochemical properties of sodium silicate crystal

The physical properties of sodium silicate crystals are shown in the pictures in Fig. 1 and some other chemical properties are in Table 1. From the images in Fig. 1, the appearance of the crystal was originally brownish white but on further washing, it became brightly white and soapy to the touch. The pH of sodium silicate solution was found to fall within the commonly reported range of 11–12.5, as a solid with alkaline properties in solution it is readily neutralized to silica solid in the presence of acid. This forms the basis for most reported work on the synthesis of silica from rice husk ash.[21,22,23,24]

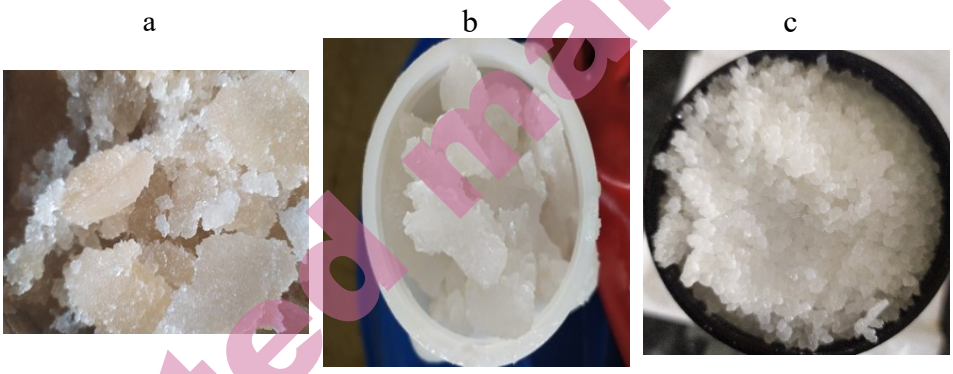

Fig. 1 Image of samples obtained (a) brownish silicate (b) washed silicate (c) crystalline appearance of washed silicate

Table 1 Some physical and chemical properties of sodium silicate crystal and silica

Samples	Sodium silicate Crystals	Sodium silicate liquor (Water glass)	750°C RHA	10% ARHA	20% ARHA
colour	Brownish to white	Brownish	white	white	white
pH	12.03	12.03	neutral	neutral	neutral
solubility/g dm^{-3}	highly	highly	insoluble	insoluble	insoluble
density / g cm^{-3}	--	1.415	---	---	---
viscosity / mPa•S	--	25	----	----	----
stability in air	slow efflorescence	stable	stable	stable	stable
melting point / °C	61	---	---	---	---
Na_2O/%	12.40	11.54	--	--	--
SiO_2/%	25.99	25.30	--	--	--
SiO_2/Na_2O	2.00	2.19	--	--	--
Total solid	38.39	36.84	--	-	-

RHA, Sodium silicate crystals composition analysis

The elemental composition of the RHA, ARHA and Sodium silicate crystals obtained from X-ray fluorescence analysis (by the air and vacuum atmosphere) are shown in Table 2. It can be noticed that the percentage composition of SiO_2 increases progressively as the acid treatment concentration increase from 10 to 20 %. While other metal oxides concentration decreases.

This indicates the effectiveness of acid treatment in purifying the rice husk ash samples, as a means of preventing unnecessary side reactions. The SiO_2 and Na_2O content of the sodium silicate crystals were 18.665 and 14.739 % respectively. This will indicate that the ratio of SiO_2 to Na_2O is 1, which is not in agreement with the classical method result. This deviation may be attributed to the consequential presence of traces of CaO, MgO, Al_2O_3, K_2O and Fe_2O_3 which might equally react with the acid during the titrimetric determination of Na_2O, thus giving a higher false value of Na_2O. According to the study by Owoeye *et al.,* the synthesis of a sodium disilicate from RHA at different concentration of 3M, 4M and 5M of NaOH was found to contains 28.64 %, 42.25 % and 36.97 % SiO_2 content while the Na_2O content was 12.32 %, 17.23 % and 18.24 % respectively[25]. Which were all higher than the 18.665 % of SiO_2 and 14.739 % of Na_2O contents obtained in the present study at lower concentration of NaOH (10 % ≡ 2.5M). Similarly, Siregar et al., reported the synthesis of sodium silicate from both corn cob and rice husk with content of Na been 43.29 % and 22.63%, that of O been 36.48 % and 71.98 % while the Si content was 20.23 % and 5.39 % respectively[26].

Table 2 EDXRF oxides composition of RHA, ARHA and Crystal

Oxides, %	750 °C RHA	10 % ARHA	20 % ARHA	Sodium silicate
Fe_2O_3	0.4698	0.15836	0.18990	0.1576
Na_2O	–	–	–	14.739
MgO	3.30	1.46	0.35	1.379
Al_2O_3	1.443	1.147	1.063	1.3516
SiO_2	72.148	90.344	91.567	18.665
P_2O_5	4.761	0.7510	0.8647	0.8505
SO_3	0.1647	0.0780	0.0777	0.3631
Cl	0.0256	0.01778	0.02052	0.0824
K_2O	3.3802	0.5772	0.5897	0.2346
CaO	0.7572	0.1326	0.1220	0.03335
MnO	0.4367	0.08555	0.08706	0.00799
SnO_2	1.00	1.00	1.00	-
others	0.17478	0.07515	0.08312	0.05111

XRD of the solid obtained

The diffractogram of RHA obtained is shown in Fig. 2. The RHA, 10 % ARHA and 20 % ARHA diffractogram pattern correspond to the mineral Cristobalite (96-900-8111). The diffractogram obtained for RHA treated at 750 °C, confirms that heat treatment of Rice husk at a higher temperature such as 750 °C

results in the formation of crystalline silica. A similar report, showed that treatment of rice husk between 450-700 °C generally results in silica predominated with amorphous phase,[27] while the higher temperature of 1000 to 1350 °C results in silica predominant by crystalline phase. Similarly, Shihab and Twej reported obtaining amorphous and crystalline phases when rice husk was treated at 650 °C and 1000 °C respectively.[24]

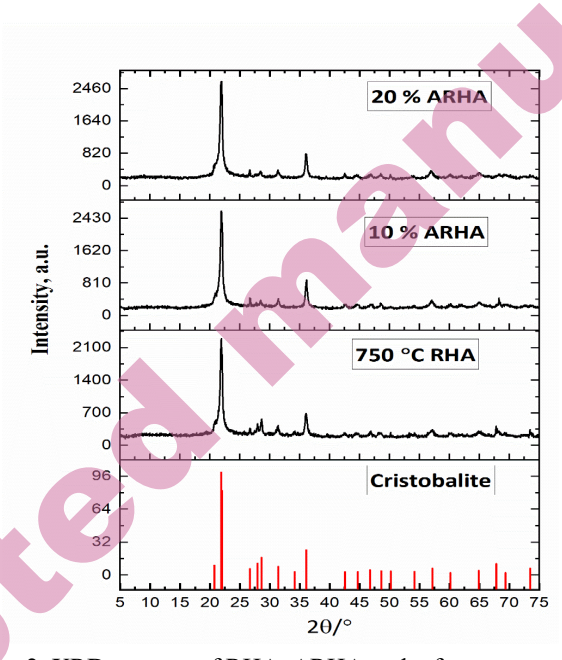

Fig. 2 XRD patterns of RHA, ARHA and reference pattern

It was also observed that there was no specific change in the crystalline phase nature of the RHA when it was acid treated at different concentrations of 10 % and 20 % HCl.

The diffractogram of the sodium silicate crystals obtained (Fig. 3) match the reference phase 2106900 of the crystallography open diffractogram with a chemical name of sodium hydrogen tetraoxosilicate heptahydrate [$Na_2(H_2SiO_4) \cdot 7H_2O$].[10]

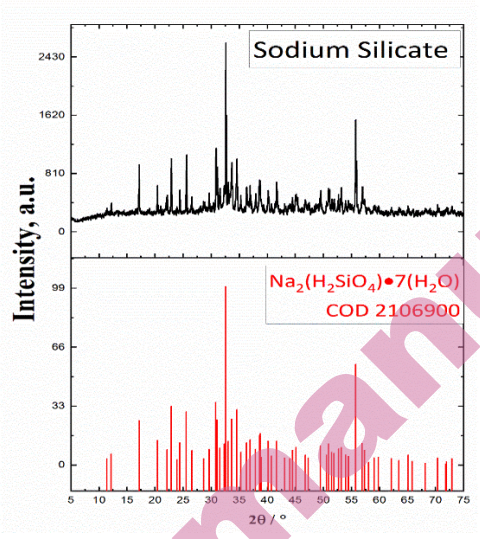

Fig.3 Diffractogram pattern of synthesized sodium silicate

The suggested properties associated with this crystal are that it is monoclinic, and the nature of its structure. Rietveld refinement of the XRD pattern for the sodium silicate performed by the profex software v5.0 gave $R_{wp} = 12.81$, $R_{exp} = 5.55$, $\chi^2 = 5.3274$, $GoF = 2.3081$ for $Na_2(H_2SiO_4)$. $7H_2O$ and $Na_3HSiO_4 \cdot 2H_2O$ phase analysis[28] (Fig. 4). The inability of the χ^2 value, to meet up to the threshold value of 1.5 may be due to the presence of some impurities (majorly Al and Mg and traces of Ca, Fe, Zn *etc.*) associated with the synthesis.

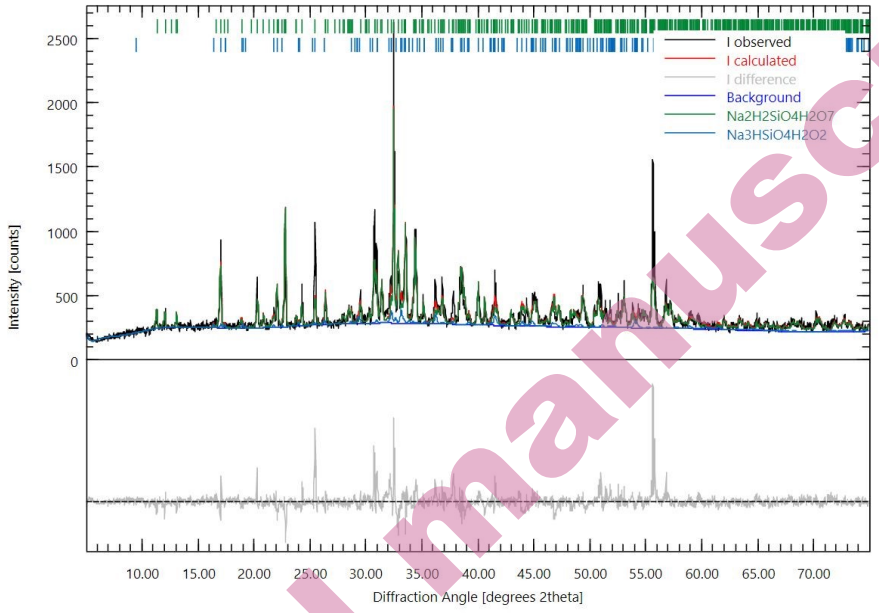

Fig. 4 Sodium silicate Rietveld refinement

FT-IR spectra of rice husk ash and sodium silicate

The infrared spectra shown in Fig. 5 of the rice husk ash treated under high temperature and acid treatment. There was very week absorption peak at position of 3000 cm^{-1} and 3500 cm^{-1} which are usually attributed to O-H group for moisture in the 750 °C RHA sample. While for 20 % ARHA and 10 % ARHA there was no visible absorption in the same region of 3000 to 3500 cm^{-1}, which is a representation of −O−H group from water or Si−O−H.[22,29] The peaks at 1021, 1098 and 1090 in 750 °C, 10 % ARHA and 20 % ARHA samples respectively are often attributed to Si−O−Si asymmetric bond stretching vibration.[30] While the peaks at 797, 794 and 795 are attributed to the Si−O bending vibration band.[31] Most of the absorption peaks detected in the 750 °C RHA sample, were also noticed to have disappeared in the 10 % ARHA and 20 % ARHA samples. This may be linked to effective removal of remnants structural lignin, cellulose and hemicellulose by the acid treatments. The spectra of sodium silicate show a strong broad peak at 3048.42 cm^{-1} which was attributed to presence of −OH group, due associated moisture. The peak at 1667.16 cm^{-1} is similarly a complementary −OH group caused by bending vibration of water[17]. While the strong stretching peak at 987.89 is due the Si−O bond stretching of the silicon tetrahedron.[32,33] The peak at 1443.94 cm^{-1} may be attributed to C−O symmetric stretching of C−O−Si, due to some C sneaked or CO_2 absorbed into the separated solid.[34] Also the peak at 2355.14 cm^{-1} position may be attributed to O=C=O stretching. The sodium silicate

crystals may have been exposed to atmospheric carbon (iv) oxide during the draining process of the crystal.

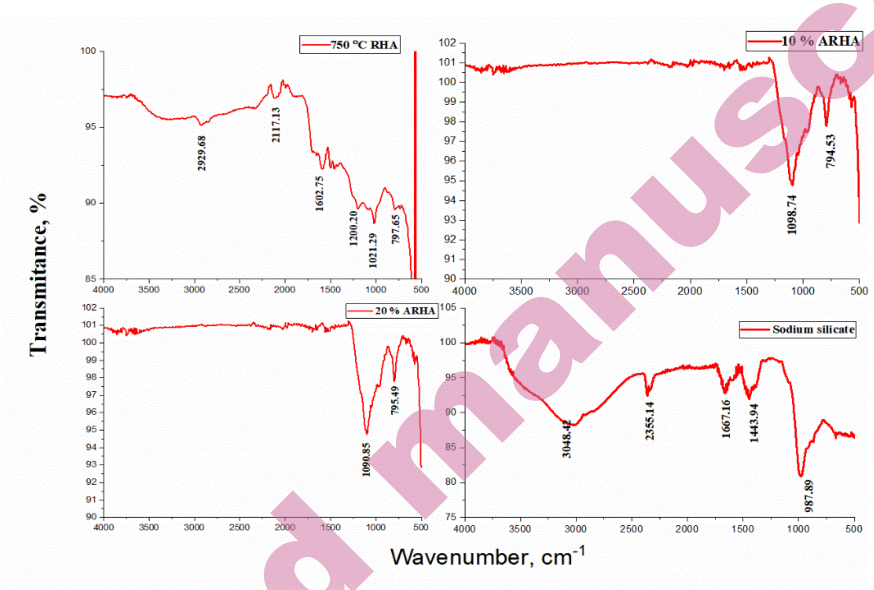

Fig. 5 Infrared spectra of sodium silicate crystals

Thermogravimetric analysis of sodium silicate crystals

The results of TGA for 750 °C RHA, 10 % ARHA, 20 % ARHA and sodium silicate crystals are shown in Fig. 6. It can be observed that a two-step weight loss occurs during the temperature treatments of RHA and 10 % ARHA. The first weight loss of 0.242 % and 0.122 % which occurs before 200 °C can be attributed to physically adsorbed water.[35] The second step weight loss occurs between 200 °C and 400 °C, which may be attributed to loss of other volatile, probably trapped in the sample's matrix during initial preparation. The sample 20 % ARHA TGA plot depicts only one step weight loss of 1.05 % between 28 °C to 450 °C. This weight loss may be attributed to release of trapped moisture as well as other volatiles. Overall the TGA of 750 °C RHA, 10 % ARHA and 20 % ARHA samples appeared to be stable to heat treatment as about 98 % of the materials remain after 850 to 900 °C.

The TGA for the sodium crystal samples show that there was also two step weight loss between 30–400 °C and between 400–500 °C. The first weight loss is considered a dehydration step, which is attributed to the loss of moisture in the crystal near and above its melting point as evidenced by the low weight loss of 1.777 %. The second, weight loss may be attributed to the removal of molar equivalents of crystal water molecules from the crystals sample as signified by the large weight loss of 34.475 %. The residue obtained after the attainment of 550 °C

is attributed to the formation of anhydrous sodium silicate. Beyond the 550 the anhydrous silicate was relatively stable with about 55 % of sample remaining.

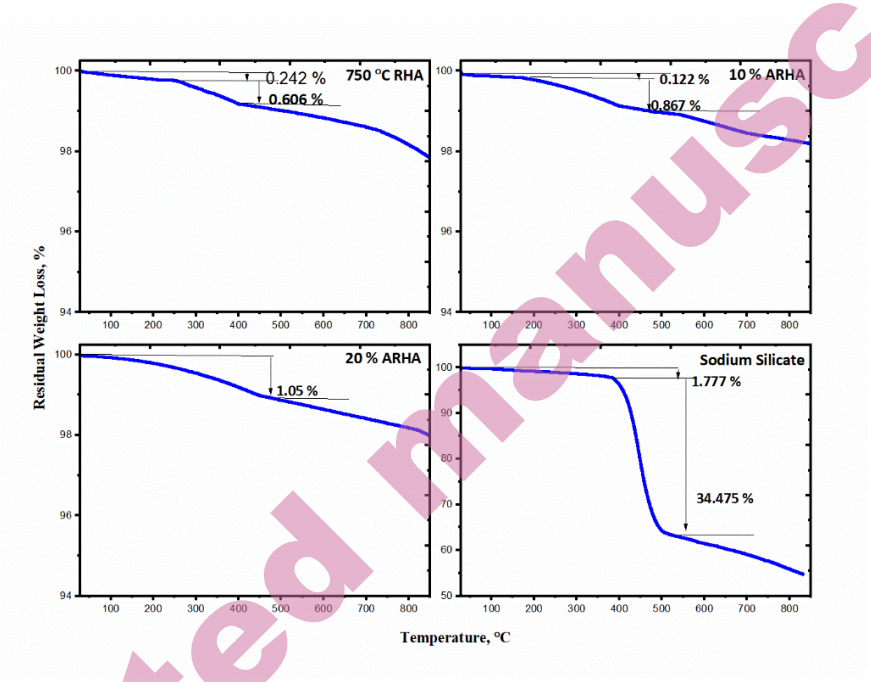

Fig. 6 Loss in weight measurement

SEM Morphological observation

The surface morphological appearance of the RHA obtained at 750 °C shows a micro-flaky and irregular shape with agglomeration. For the 10 % ARHA the micro flaky agglomeration possesses a wavy opening fitted with lateral pores much like an oval hexagon and the 20 % ARHA showed no wavy pattern opening while also showing rod-like microstructure and some micropores. The isolated rod-like structure seen in the 20 % ARHA bears evidence of induced crystallinity as a result of increased acid concentration. The sodium silicate morphology at 12000× magnification Figure 7d, shows an uneven surface and the appearance of tiny pores on the surface of agglomerated morphology. The surface of the crystal also appears to have slight indentation while the irregular pores appears to run deep.

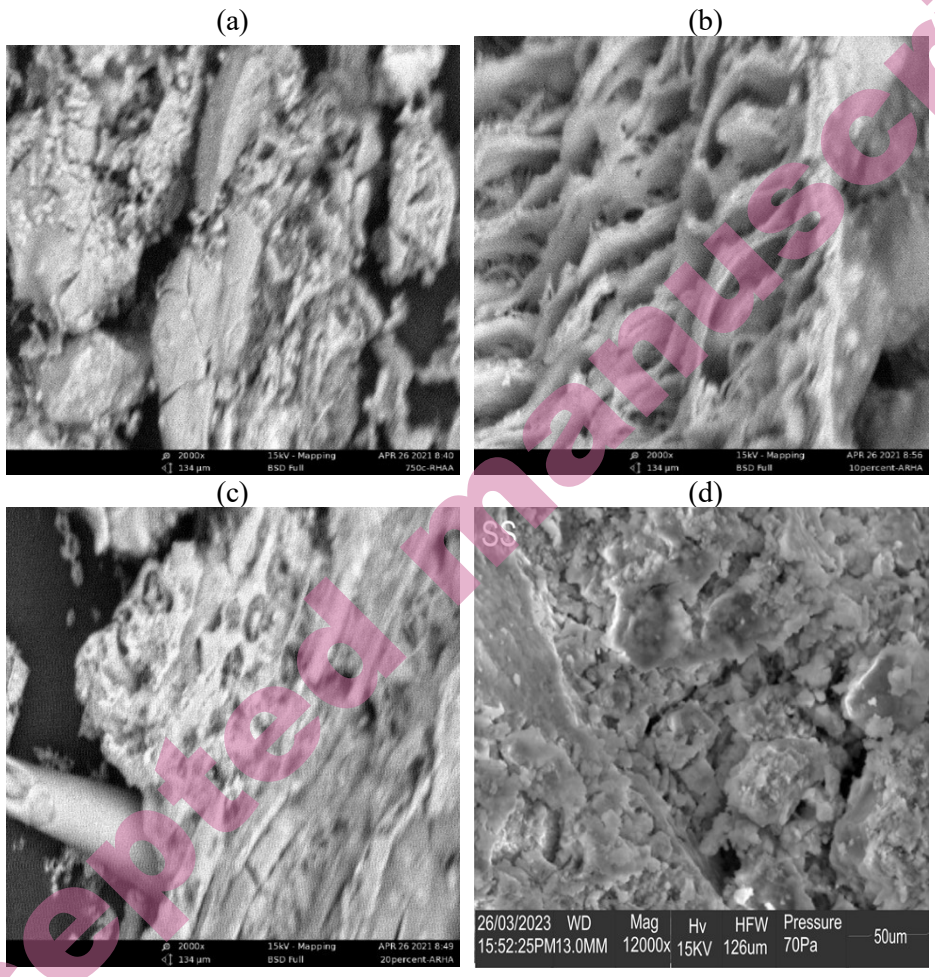

Fig. 7 Scanning electron microscopic image of (a) 750 °C RHA, (b) 10 % ARHA, (c) 20 % ARHA, (d) sodium silicate (SS) crystal surface

Significant agglomeration of particles on the surface of the amorphous silica, used in the synthesis of sodium silicate from corncob and rice husk as well as existence of pores within the agglomerates was similarly reported.[26]

CONCLUSION

Rice husk ash was used to synthesize crystalline sodium silicates. The acid treatment of RHA showed improvement on the purification of silica obtained as well as improved crystal structure. The similarity of all the RHA (750 °C, 10 % ARHA and 20 % ARHA) to the cristobalite phase also shows that treatment type, affects the crystallinity of the silica obtained. The sodium silicate sample synthesized was found to contain two phases namely disodium orthosilicate

(91.91 % $Na_2H_2SiO_4 \cdot 7H_2O$) and trisodium orthosilicate (8.10 % $Na_3HSiO_4 \cdot 2H_2O$), as revealed by the rietveld refinement analysis. Since disodium orthosilicate are often used in cosmetic formulations as an exfoliating agent or abrasive. The synthesized orthosilicate will be useful in improving skin texture when added to cosmetics.

Conflict of interest: The authors declare that there is no conflict of interest regarding the publication of this paper.

Acknowledgement: This work was supported by the Raw Material Research and Development Council of Nigeria.

LIST OF SYMBOLS AND ABBREVIATIONS

ARHA- Acid treated rice Husk Ash
ATR- Attenuated total reflectectance
BSCA-Brownish Silicate Crystal Abuja
COD- Crystallography Open Database
DTA-Differential Thermal Analysis
EDXRF- Energy-dispersive X-ray fluorescence spectrometer
FAO-Food and Agriculture Organization
FTIR-Fourier Transform Infra-red spectrophotometer
RMRDC-Raw Materials Research and Development Council
RHA - Rice Husk Ash
SEM- Scanning Electron Microscope
SHESTCO- Sheda Science and Technology Complex
TGA- Thermogravimetry Analysis
XRD-X-ray Diffraction/Diffractometer
R_{wp} – Weight Profile R- Factor
R_{exp} – Expected R Factor
GoF – Goodness of Fit

И З В О Д

СИНТЕЗА КРИСТАЛА НАТРИЈУМ-СИЛИКАТА ИЗ ПЕПЕЛА ПИРИНЧАНЕ ЉУСКЕ

STELLA ADEDUNNI EMMANUEL[1], ALHASSAN ADEKU SALLAU[1]*, OLUWASEYE ADEDIRIN[1], HUSSAIN DOKO IBRAHIM[2], MOHAMMED LAWAL BUGA[2], ANTHONY OKEREKE[2], GERTRUDE NGOZI OZONYIA[2] И FORTUNE MIEBAKA ALABI[2]

[1]Chemistry Advanced Research Center, SHESTCO, Abuja, Nigeria, и [2]Raw Materials Research and Development Council, RMRDC, Maitama, Abuja

Због узгоја пиринча широм света пиринчана љуска представља веома распрострањени пољопривредни отпад богат аморфним силицијумом. У овом раду пиролизом на 750 °C пиринчана љуска је претворена у бели пепео (RHA), који је затим третиран киселином (ARHA). Након тога, добијена суспензија је реагована са натријум-хидроксидом на 90 °C за време од 2,5 сата, при чему долази до издвајања кристала натријум-силиката. Кристали натријум-силиката су окарактерисани на бази различитих физичко-хемијских параметара. За одређивање структуре силиката употребљени су

инфрацрвени спектрофотометар са Фуријевом трансформацијом (FTIR), рендгенски дифрактометар (XRD) и микроскоп са скенирајућим електродама (SEM). За испитивање минералошког састава пепела и натријум-силиката коришћен је енергетски дисперзивни рендгенски флуоресцентни спектрометар (EDXRF). Тачка топљења добијених кристала натријум-силиката је 61 °C, pH = 12,03, док је њихова боја била између светлосмеђе и светлосиве. Рендгенско-структурна испитивања (XRD) белог пепела, након његове реакције са киселином (ARHA), су показала да испитивани узорци одговарају структури минерала кристобалита, док структура натријум-силиката одговара структури минерала натријум-триоксосиликат хептахидрат. Методом утачњавања (Rietveld refinement method) за кристале натријум-силиката добијене су следеће вредности: R_{wp} = 12.81, R_{exp} = 5.55, χ^2 = 5.3274 и GoF = 2.3081. Нађено је да су кристали натријум-силиката погодни за припрему козметичких формулација.

(Примљено 22. августа 2022; ревидирано 2. октобра 2022; прихваћено 10. јула 2023.)

REFERENCES

1. S. A. Ajeel, K. A. Sukkar, and N. K. Zedin, *IOP Conf. Ser.: Mater. Sci. Eng.* **881** (2020) 012096 (https://doi.org/10.1088/1757-899X/881/1/012096)
2. K. T. Tong, R. Vinai, & M. N. Soutsos, *J. Clean. Prod.* **201** (2018) 272–286 (https://doi.org/10.1016/j.jclepro.2018.08.025)
3. H. Gandhi, A. N. Tamaskar, H. Parab, & S. Purohit, *J. Basic Appl. Eng. Res.* **2** (2015) 330–333 (https://www.krishisanskriti.org/vol_image/07Jul2015100713xxHeta%20Gandhi%20%20%20%20%20%20%20%20%20%20%20%20%20%20%20%20%20%20%20%20%20330-333.pdf)
4. S. S. Owoeye & O. E. Isinkaye, *Sci. J. Chem.* **5** (2017) 8–11 (https://doi.org/10.11648/j.sjc.20170501.12)
5. G. T. Adylov, S. A. Faiziev, M. S. Paizullakhanov, S. Mukhsimov, & É. Nodirmatov, *Tech. Phys. Lett.* **29** (2003) 221–223 (http://dx.doi.org/10.1134/1.1565639)
6. M. K. Omatola and D. A. Onojah, *Int. J. Phy. Sci.* **4** (2009)189-193 (http://www.academicjournals.org/ijps/PDF/pdf2009/April/Omotola%20and%20Onoja h.pdf)
7. R. V Krishnarao, J. Subrahmanyam, & T. J. Kumar, *J. Eur. Ceram. Soc.* **21** (2001) 99–104 (https://doi.org/10.1016/S0955-2219(00)00170-9)
8. A. Mehta & R. P. Ugwekar, *IJERA*. **5** (2015) 43–48 (https://www.ijera.com/papers/Vol5_issue8/)
9. H. Engelhardt & L. E. Von Borstel, *Z. Dtsch. Ges. Grundwasser* **165** (2020) 115 (https://doi.org/10.1127/1860-1804/2014/0057)
10. N. V. Zubkova, I. V. Pekov, D. Yu. Pushcharovsky, *Min. Mag*. **78** (2014). 253-265 (https://doi.org/10.1180/minmag.2014.078.2.03)
11. V. Kahlenberg, *Min. Chimia*. **64** (2010) 716–722 (https://doi.org/10.2533/chimia.2010.716)
12. M. Mcdonald and X. Li, *AADE Fluids Tech. Conf. & Exh.(2014)* 2014, pp. 1–6 (https://www.aade.org/download_file/2069/420)
13. M. Adamu, J. O. Okafor, & G. T. David, *J. Sci. Technol. Math. Educ.* **11** (2015) 163–170 (https://jostmed.futminna.edu.ng/image/JOSTMED/Jostmed_11_2_August_2015)

14. J. X. Dong, L. P. Li, H. Xu, F. Deng, G. Y. Zhang, J. P. Li and X. J. Ai, *Tenside Surf. Det.* **44** (2007) 34 (https://doi.org/10.3139/113.100326)
15. S. Yunusa, I. A. Mohammed-Dabo and A. S. Ahmed, *Int. J. Sci. Eng. Res. Vol.* **6** (2015) 1183–1191 (http://www.ijser.org)
16. J. L. Thompson, B. E. Scheetz, M. R. Schock, & D. A. Lytle, ***Pro. AWWA Wat. Qua. Tech. Conf.*** 9(1997). (https://aniq.org.mx/pdf)
17. G. K. Sharma, J. Gadiya and M. Dhanawat (2018). Textbook of Cosmetic Formulations. (https://www.researchgate.net/publication/325023106)
18. E. L. Foletto, E. Gratieri, L. H. Oliveira, and S. L. Jahn, *Materials Research* **9** (2006) 335-338 (https://doi.org/10.1590/S1516-14392006000300014)
19. Y. Shen, P. Zhao and Q. Shao, *Microporous and Mesoporous Materials* **188** (2014) 46-76 (https://doi.org/10.1016/j.micromeso.2014.01.005)
20. X. Liu, Z. Li, H. Chen, L. Yang, Y. Tian and Z. Wang, *Res. Chem. Intermed.* **42** (2015) 3887-3903 (https://doi.org/10.1007/s11164-015-2251-7)
21. J. Monzo, M. V Borrachero, A. Mellado, L. M. Ordon, & J. Paya, *Cem. Concr. Res.* **31** (2001) 227–231 (https://doi.org/10.1016/S0008-8846(00)00466-X)
22. R. Patil, R. Dongre, & J. Meshram, *IOSR J. Appl. Chem.* **2014** (2014) 26–29 (https://www.iosrjournals.org/iosr-jac/papers/ICAET-2014/volume-1/6.pdf)
23. *G. V. V. Gowthami, A. Sahoo*, P. Thesis, (2015). (http://ethesis.nitrkl.ac.in/6867/1/Preparation_Gowthami_2015.pdf)
24. B. F. Shihab, *Iraq. J. Phys.***16** (2018) 117–123 (https://doi.org/10.30723/ijp.v16i39.109)
25. S. S. Owoeye, S. M. Abegunde and B. Oji. *Global J. Eng. & Tech. Adv.* **06**(01) (2021) 066–075 (https://doi.org/10.30574/gjeta.2021.6.1.0001)
26. A. G. A. Siregar, R. Manurung and T. Taslim, *Indones. J. Chem.* **21** (2021) 88–96 (https://doi.org/10.22146/ijc.53057)
27. E. L. Foletto, E. Gratieri, L. H. De Oliveira, S. L. Jahn, *Mat. Res*. **9** (2006) 335–338 (https://doi.org/10.1590/S1516-14392006000300014)
28. N. Döbelin and R. Kleeberg, *J. Appl. Crystallogr.* **48** (2015) 1–8 (https://doi.org/10.1107/S1600576715014685)
29. I. U. Haq, K. Akhtar, & A. Malik, *J. Chem. Soc. Pak.***36** (2014) 382–387 (https://www.researchgate.net/publication/286071234)
30. P. Taylor, J. P. Nayak, & J. Bera, *Trans. Indian Ceram. Soc.* **68** (2015) 37–41 (https://doi.org/10.1080/0371750X.2009.11082163)
31. I. M. Joni, L. Nulhakim, M. Vanitha, C. Panatarani, *J. Phys. Conf. Ser.* **1080** (2018) 012006 (https://doi.org/10.1088/1742-6596/1080/1/012006)
32. L. Fernández-Carrasco, D. Torrens-Martín, L.M. Morales, and Sagrario Martínez-Ramírez, in 'Infrared Spectroscopy - Materials Science, Engineering and Technology, ed. T. Theophanides. InTech 2012 (https://doi.org/10.5772/36186)
33. C. Kongmanklang & K. Rangsriwatananon, *Journal of Spectroscopy; Spectroscopy in Materials Chemistry* ed. Nikša Krstulović, **2015** (2015) 696513 (https://doi.org/10.1155/2015/696513)
34. J. Coates, in *Encyclopedia of Analytical Chemistry,* R.A. Meyers (Ed.) 10815–10837 John Wiley & Sons Ltd, Chichester, 2000 (https://analyticalscience.wiley.com/do/10.1002/sepspec.10120education/full/i97dca9608c7bfa88fcf79f9b29f68226.pdf)
35. P. E. Imoisili, K. O. Ukoba, & T. Jen, *Boletín de la Sociedad Española de Cerámica y Vidrio* **59** (2020) 159–164 (https://doi.org/10.1016/j.bsecv.2019.09.006).